Mechanism and dynamics of biexciton formation from a long-lived dark exciton in a CdTe quantum dot

T. Smoleński,[1,*] T. Kazimierczuk,[1,†] M. Goryca,[1] P. Wojnar,[2] and P. Kossacki[1]

[1]*Institute of Experimental Physics, Faculty of Physics, University of Warsaw, ul. Pasteura 5, 02-093 Warsaw, Poland*

[2]*Institute of Physics, Polish Academy of Sciences, Al. Lotników 32/64, 02-688 Warsaw, Poland*

(Received 4 March 2015; published 27 April 2015)

We study the biexciton formation process in a single CdTe/ZnTe quantum dot. Consistently with previous studies, we find subquadratic dependence of the biexciton photoluminescence intensity on the excitation power. We quantitatively explain this dependence in terms of the interplay between two alternative biexciton formation mechanisms, including the formation from a long-lived dark exciton residing in the quantum dot. This mechanism is demonstrated to be a dominant one for a wide range of excitation intensities. Our study is complemented by determination of a characteristic biexciton formation time, which is shown to be governed by the spin relaxation dynamics of an excited electron pair.

DOI: 10.1103/PhysRevB.91.155430 PACS number(s): 78.67.Hc, 78.47.jd, 78.55.Et

I. INTRODUCTION

Numerous optical studies of various quantum dot (QD) systems established a toolbox of techniques particularly effective in characterization of single-dot photoluminescence (PL) spectra. Photon autocorrelation measurement is used to demonstrate that the QD is a single quantum emitter [1–3]. Photon cross-correlations uncover relationships between different lines, e.g., cascadelike arrangement [4–7]. Polarization-resolved PL measurements typically reveal excitonic fine structure [8], distinguishing between neutral states affected by anisotropic exchange splitting and singly charged states, which do not exhibit such a splitting. Finally, there is a measurement of the PL spectrum as a function of the excitation intensity, which is employed to distinguish between excitons, biexcitons, and higher multiexcitonic complexes [9].

The results obtained using the last of those techniques—PL measurements as a function of the excitation intensity—are usually discussed in terms of a power-law behavior of the PL intensity, both in the pulsed and continuous-wave (CW) excitation regimes. The simplistic stochastic model states that the formation of the biexciton requires a coincidence of two exciton formation events [10], and thus the exciton PL intensity should increase linearly with the excitation power, whereas the biexciton PL intensity should be quadratic. In real experiments the biexciton PL intensity often does not follow this prediction and exhibits less steep dependence [7,11–18]. Such a deviation from quadratic dependence is of no interest regarding the identification of the biexciton state, since its PL intensity is still superlinear. However, a more detailed analysis can provide some new insight into the complex problem of a QD excitation mechanism under nonresonant (incoherent) excitation.

In this work we analyze the excitation intensity dependence of a single QD PL with respect to the biexciton formation process. We demonstrate that in the wide range of excitation intensities the key mechanism is the formation of a biexciton from a dark exciton. Such an exciton exhibits long (up to microseconds) lifetime, since its radiative recombination is only allowed by perturbations such as in-plane magnetic field [8,19], valence-band mixing [20–22], or QD shape imperfection [23,24]. As such, a long-lived dark exciton state can store a photoexcited electron-hole pair until another electron-hole pair is injected resulting in a biexciton formation. A primary consequence of this mechanism is nonquadratic excitation power dependence of the biexciton PL intensity.

The discussed mechanism opens interesting possibilities due to the fact that two electron-hole pairs forming a biexciton are excited by different laser pulses, which can be controlled independently. In particular, we exploit it to study an effect of carrier spin polarization on the dynamics of biexciton formation. Our results evidence that the dynamics of this formation is mainly governed by the effect of the electron spin blockade.

II. EXPERIMENTAL DETAILS

A. Sample and experimental setup

The sample studied in this work contains a molecular beam epitaxy grown single layer of self-organized CdTe QDs embedded in a ZnTe barrier. The optical experiments were performed in a microphotoluminescence setup with the sample immersed in superfluid helium ($T = 1.8$ K) inside a magneto-optical cryostat. The QDs were excited below the band gap of the ZnTe barrier. In the initial stage of a QD characterization we used a CW rhodamine 6G dye laser, while in all other experiments we employed a pulsed optical parametric oscillator (OPO). Both of the lasers were tunable from 560–600 nm. The pulses emitted by the OPO were spectrally narrowed with an etalon. For some of the measurements a nominal OPO repetition rate of 76 MHz was reduced with a pulse picker. It allowed us to define the pulse separation time by picking certain pulses and blocking all the others with a contrast ratio better than 100:1.

To allow the studies of single QDs, the laser beam was focalized to a spot of a diameter smaller than 1 μm with the use of a reflective-type microscope objective attached directly to the sample surface. The QDs PL was resolved with a monochromator and recorded either by a CCD camera or, in the case of time-resolved measurements, by a Hamamatsu

*tomasz.smolenski@fuw.edu.pl

†tomasz.kazimierczuk@fuw.edu.pl

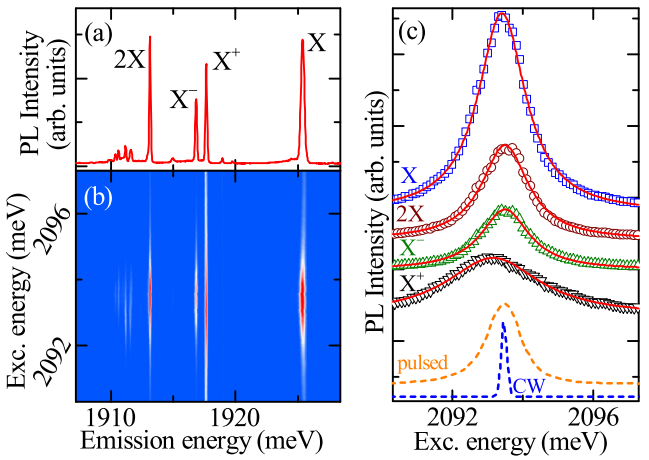

FIG. 1. (Color online) (a) PL spectrum of a single QD excited at the resonance and (b) corresponding PLE map. (c) PLE spectra of the same QD measured for various emission lines (as indicated). Solid lines represent the fitted Lorentzian profiles. The spectra are shifted vertically for clarity. Dashed lines present the spectra of a CW dye laser used in the PLE measurements and pulsed OPO used in the rest of the work.

synchroscan streak camera providing temporal resolution of about 10 ps.

B. Optical excitation technique

Our experiments were performed on a number of randomly selected CdTe/ZnTe QDs. A PL spectrum of a representative one is presented in Fig. 1(a). It exhibits a well-established emission pattern [25,26], which consists of four lines originating from the recombination of a neutral exciton (X), charged excitons (X^+, X^-), and biexciton (2X). The presence of the lines related to excitonic complexes of different charge states in the time-integrated spectrum indicates existence of the QD charge-state fluctuations. Their dynamics has been extensively studied in the previous experiments [7,27–29] and was found to be strongly dependent on actual excitation conditions. In particular, under pulsed nonresonant excitation the most efficient QD excitation channel was ascribed to the single-carrier trapping [7,28], which implies that the QD charge-state variation occurs statistically after each laser pulse. In this work, to reduce the influence and relative dynamics of these charge fluctuations, we employ below-the-barrier excitation. It is realized by taking advantage of a natural tendency of self-assembled CdTe/ZnTe QDs to form spontaneously coupled pairs, between which an efficient exciton transfer is observed [27,30–32]. Experimentally, we select a QD exhibiting a relatively sharp resonance in the photoluminescence-excitation (PLE) spectra, as shown in Fig. 1(b). Such a resonance originates from an absorption in an adjacent QD, from which the optically created excitons tunnel out and are transferred to the studied dot, where they recombine.

The PLE spectra of different emission lines from the emitting QD measured with a CW dye laser are presented in Fig. 1(c). Each of them exhibits homogeneous broadening related to a short excitonic lifetime in the absorbing dot. In case of the presented QD, such lifetime is determined to be about 0.4 ps based on the energy width of the Lorentzian profiles fitted to PLE spectra of the X, X^-, and 2X transitions. For each of these transitions the energy of the resonance is similar and yields about 2093.5 meV, which corresponds to the excitonic energy in the absorbing dot. In contrast, for the X^+ emission line the resonance energy is red shifted by ∼0.3 meV and the absorption line is about two times wider. Such an effect was also observed in the previous studies on coupled CdTe QDs [27] and is most probably related to the influence of weakly confined hole residing in the emitting dot on the energy and lifetime of resonantly created exciton in the absorbing QD.

In the following part we will focus on the experiments performed under pulsed excitation with the OPO tuned to the X resonance. The temporal width of the pulse is determined to be about 0.6 ps based on its spectral width [see Fig. 1(c)]. Since this value is large compared to the excitonic lifetime in the absorbing dot, we do not observe any coherent effects, e.g., Rabi oscillations. At the same time, under such excitation the events of single-carrier trapping are more than an order of magnitude less frequent compared to the injection of resonantly created electron-hole pairs, as was evidenced in Ref. [27]. Thus, we will neglect the QD charge-state fluctuations in further analysis.

III. TWO MECHANISMS OF 2X FORMATION

The 2X formation mechanisms are studied by measurements of X and 2X PL intensity dependence on the power P of the pulsed excitation. The results are shown in Fig. 2(a). As expected, the X intensity initially increases roughly linearly with the excitation power. However, the dependence obtained for the 2X is far from being quadratic, which is a prediction of the typically invoked scenario of the 2X formation from two excitons injected to an empty dot by a single laser pulse [10]. Subquadratic increase is naturally expected in the saturation regime, but we observe it also for significantly lower excitation intensities. In fact, the actual dependence of the 2X PL intensity on the excitation power in the moderate power range ($1\ \mu W/\mu m^2 \lesssim P \lesssim 10\ \mu W/\mu m^2$) is close to a linear one. This observation implies the importance of another 2X formation mechanism, which we identify as related to the dark exciton (DX). Such an exciton is likely to be injected to the QD owing to any spin flip of an electron or a hole occurring during the transfer of an optically created exciton between the coupled dots. Crucially, the lifetime of the dark exciton in a CdTe/ZnTe QD is much longer compared to the pulse separation time of 13.2 ns [21]. As a result, once the DX emerges in the dot, it will most probably reside there until another exciton will be injected. This will finally lead to the 2X formation. Importantly, such a formation mechanism is expected to exhibit linear excitation power dependence, as its only prerequisite is the previous formation of a dark exciton.

The analysis presented above provides a qualitative understanding of the measured dependence of the 2X PL intensity on the excitation power. In order to gain a better insight into the relative efficiencies of two possible 2X formation mechanisms, we analyze the relative probabilities p_X and p_{2X} of X and 2X occupation by a single laser pulse. Their values, however, are not directly reflected by the respective PL intensities due to a

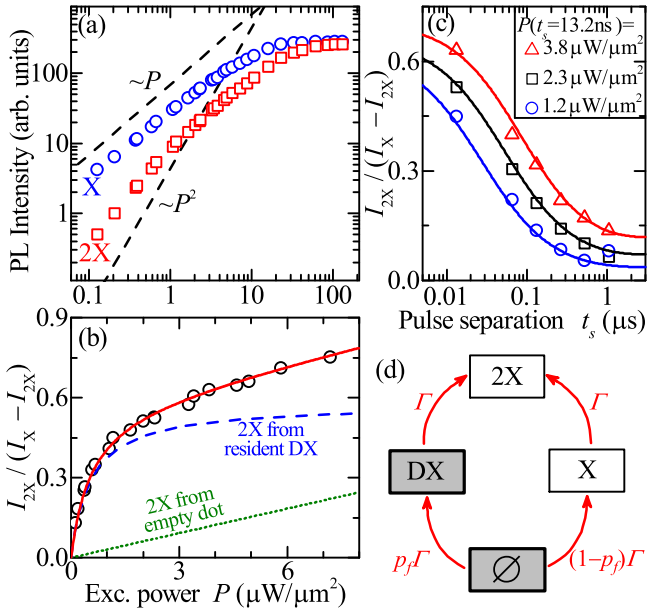

FIG. 2. (Color online) (a) Integrated PL intensities of X and 2X versus pulsed excitation power. Dashed lines representing the linear and quadratic dependences are drawn for the reference. (b) The ratio $I_{2X}/(I_X - I_{2X})$ versus pulsed excitation power (repetition rate 76 MHz). The solid line corresponds to the fitted curve described by Eq. (1), while dashed and dotted lines represent the contributions from two 2X formation mechanisms (as indicated). (c) The ratio $I_{2X}/(I_X - I_{2X})$ measured as a function of the pulse separation time (i.e., pulse repetition rate) keeping pulse intensity constant. Each set of data points corresponds to different pulse power (as indicated). Solid lines represent the fitted curves given by Eq. (1). (d) Scheme of QD states and optical excitation transitions considered in the rate-equation model with indicated integrated probabilities of each excitation transition (recombination transitions not shown). The states labeled with gray rectangles (empty dot ∅ and dark exciton DX) are stable at the scale of 13.2 ns, while the states denoted with white rectangles (X and 2X) are emptied completely during 13.2 ns due to the radiative recombination.

cascade nature of the 2X recombination process, which leaves the bright exciton in the dot. In general, the bright exciton at this stage might nonradiatively relax to the dark exciton state. Such a relaxation would lead, for example, to the 2X saturation at the higher level as compared to the X [12,13,33–35]. We find no signature of such an effect in our experimental data and therefore assume that 2X recombination is always followed by the X emission. Consequently, the ratio p_{2X}/p_X is given by $I_{2X}/(I_X - I_{2X})$, where I_X and I_{2X} denote the PL intensities of X and 2X, respectively. The dependence of this ratio on the excitation power is shown in Fig. 2(b). To avoid the saturation effects, the presented data correspond to a low-to-moderate power range ($P < 8\ \mu\mathrm{W}/\mu\mathrm{m}^2$). At $P \gtrsim 1\ \mu\mathrm{W}/\mu\mathrm{m}^2$ we observe almost linear increase of p_{2X}/p_X with the excitation power. The linear slope reflects a quadratic contribution to p_{2X} power dependence. Such a contribution is identified with a well-known 2X formation mechanism from an empty dot by a single laser pulse. However, the measured power dependence of p_{2X}/p_X exhibits also a pronounced constant offset, which in turn corresponds to a linear contribution to p_{2X} increase with the excitation power. This is a direct fingerprint of the second 2X formation mechanism related to a long-lived dark exciton. As seen in Fig. 2(b), this mechanism is dominant in the analyzed power range and its relative contribution is progressively increasing for lower excitation powers owing to a decreased probability of the 2X formation from an empty dot. For example, at $P = 2\ \mu\mathrm{W}/\mu\mathrm{m}^2$ about 90% of the biexcitons are created from resident dark excitons. Interestingly, at very low powers ($P \lesssim 1\ \mu\mathrm{W}/\mu\mathrm{m}^2$) even the efficiency of the DX-related mechanism is decreasing, which underlies the observed decrease of the p_{2X}/p_X ratio. This effect occurs for very small probabilities of a laser pulse absorption when the average time between two consecutive events of an exciton injection to the QD becomes comparable with the dark exciton lifetime. In such a case, the DX is recombining prior to the injection of the second exciton, and thus it cannot participate in the 2X formation. The effect of similar nature can be also independently studied in the experiment in which the pulse intensity remains constant, but the pulse separation time t_s is increased with the use of the pulse picker. The measured dependences of $I_{2X}/(I_X - I_{2X})$ on t_s for three different pulse intensities are presented in Fig. 2(c). As expected, for longer delay between pulses the probability of DX recombination increases, which gives rise to a decrease of the p_{2X}/p_X ratio observed for each pulse intensity. It is noteworthy that this effect originates solely from decreasing contribution of DX-related mechanism to the 2X formation, since the efficiency of the second mechanism corresponding to the 2X formation from an empty dot is naturally independent of t_s.

The quantitative description of all our experimental results is provided by a simple rate-equation model. It includes four QD states, which are schematically depicted in Fig. 2(d). We consider pulse separation times $t_s \geqslant 13.2$ ns, which are much longer compared to X and 2X radiative lifetimes in a CdTe/ZnTe QD [16,36]. Hence, we assume that both of these complexes always recombine radiatively during t_s. On the other hand, the lifetime τ_{DX} of the DX is taken as a free parameter. We also introduce a constant p_f corresponding to a probability that an optically created exciton flips its spin during the interdot transfer and is eventually injected to the QD as a dark one. Finally, we assume that exciton injection after a laser pulse is much faster compared to all excitonic lifetimes [27], and that the integrated probability Γ of an exciton creation in the higher-energy dot is independent of the actual occupation of the lower-energy QD. Under these assumptions we can derive an analytical formula describing the ratio p_{2X}/p_X in a steady state, which in the low-power regime (i.e., when $\Gamma \ll 1$ is proportional to the excitation power) reads

$$\frac{p_{2X}}{p_X} = \frac{I_{2X}}{I_X - I_{2X}} = \frac{\Gamma}{2(1-p_f)} + \frac{p_f}{(1-p_f)} \frac{\Gamma}{\left[\exp\left(\frac{t_s}{\tau_{DX}}\right)(1+\Gamma) - 1\right]}, \quad (1)$$

where the first term corresponds to 2X formation from an empty dot, while the second is related to the formation from the DX. The above formula accurately reproduces the data from Figs. 2(b) and 2(c) for the same set of parameters. The DX lifetime τ_{DX} determined from the fit yields 620 ns, which

is consistent with the results of direct time-resolved measurements from Ref. [21]. The probability p_f is in turn almost directly obtained based on the p_{2X}/p_X ratio corresponding to the saturation of DX-related 2X formation mechanism [dashed line in Fig. 2(b)], which is equal to $p_f/(1-p_f)$. The determined p_f of about 37% indicates quite high probability of bright-to-dark exciton spin flip during the transfer between the coupled QDs and subsequent energy relaxation. At the same time, such excitation regime is characterized by high circular polarization transfer efficiency (up to 70%), as already reported previously in Refs. [27,30] and independently confirmed in the present study. This observation suggests that only one out of two carriers forming the exciton keeps its spin during the interdot transfer, while the other carrier becomes significantly depolarized. Such an effect has been previously observed in other QD systems, e.g., in InAs/GaAs QDs pumped via the wetting layer, in which only the electron was found to conserve its spin based on the analysis of the negative X^- optical orientation [37,38]. Similar efficiency of this process in CdTe/ZnTe QDs [27] might thus indicate that such an explanation is also valid in case of the studied dots.

IV. DYNAMICS OF 2X FORMATION

In order to have more complete insight into the 2X formation process, we study its dynamics by means of time-resolved measurements of the QD emission under pulsed excitation. As we show later in this section, the 2X formation dynamics is governed by the spin blockade between relaxing carriers. To corroborate this claim and identify which carriers are relevant for the blockade effect, we investigate simultaneously the formation dynamics of all four excitonic complexes present in a CdTe/ZnTe QD PL spectrum. These experiments are carried out upon application of low magnetic field of 1.5 T in the Faraday configuration, which is needed to purify the exciton spin states in the absorbing QD [27], and thereby to achieve the control over the spin of excitons injected to the lower-energy dot. The time-dependent PL intensities measured with a streak camera for various excitonic complexes are shown in Fig. 3(a). Each of them is characterized by a relatively fast rise, which is followed by a slower decay. The decay dynamics is governed solely by the respective radiative lifetime. On the other hand, the time scale of the PL rise corresponds to a characteristic formation time of a given excitonic complex in its ground state. Interestingly, we observe a pronounced difference between the PL rise dynamics for various complexes: the PL of X and X^+ reaches its maximum value almost instantly after a laser pulse, whereas the X^- and 2X PL continues to rise for about 100 ps.

To perform a quantitative analysis of the formation dynamics, we assume that the ground-state occupation probability $p(t)$ for a given excitonic complex at the time t after a laser pulse is determined by $dp(t)/dt = \gamma(t) - p(t)/\tau$, where τ denotes the radiative lifetime, while $\gamma(t)$ corresponds to the time-dependent formation probability. Its integral $\Gamma(t) = \int_0^t \gamma(t')dt'$ can be thus expressed (up to the normalization constant) with the use of the time-resolved PL intensity $I(t) \propto p(t)/\tau$ and reads

$$\Gamma(t) = I(t)\tau + \int_0^t I(t')dt'. \qquad (2)$$

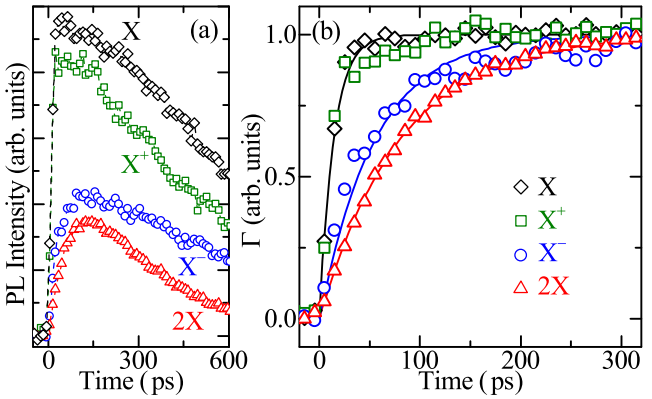

FIG. 3. (Color online) (a) PL dynamics of X, X^+, X^-, and 2X measured at $B = 1.5$ T under σ^- polarized pulsed excitation. Each of the temporal profiles is determined as a sum of two profiles detected in orthogonal circular polarizations and rescaled for better visibility. (b) Normalized integrated formation probabilities Γ of four excitonic complexes versus time t after a laser pulse arrival. Solid lines represent the fitted curves of the form $\Gamma(t) \propto 1 - \exp(-t/\tau^{\mathrm{exc}})$ with $\tau_X^{\mathrm{exc}} \approx \tau_{X^+}^{\mathrm{exc}} = 14$ ps, $\tau_{X^-}^{\mathrm{exc}} = 55$ ps, and $\tau_{2X}^{\mathrm{exc}} = 80$ ps.

Such a formula applies to each excitonic complex observed in the QD PL spectrum except the neutral exciton, for which one should additionally take into account the contribution from the cascaded 2X recombination. It is explicitly done by subtracting the integral $\int_0^t I_{2X}(t')dt'$ of the 2X PL intensity from the right side of Eq. (2). The radiative lifetimes, being the only parameters of the described model, are independently determined from the time-resolved PL measurements performed at a longer time scale of about 2 ns and yield $\tau_X = 410$ ps, $\tau_{X^+} = 580$ ps, $\tau_{X^-} = 600$ ps, and $\tau_{2X} = 250$ ps.

The above approach allows us to obtain the time-dependent integrated formation probabilities $\Gamma(t)$ for each excitonic complex based on the data in Fig. 3(a). The results are shown in Fig. 3(b). They are well described by dependences of the form $\Gamma(t) \propto 1 - \exp(-t/\tau^{\mathrm{exc}})$, which corresponds to anticipated [7,28] exponential profile of the formation probability $\gamma(t)$ starting at the time of a laser pulse arrival and decaying with a time constant τ^{exc}. On this basis we determine the effective formation times τ^{exc} for various complexes. In the case of the X and X^+ they are similar and equal to about 14 ps, which is close to the temporal resolution of our experimental setup and might be regarded as an upper bound. On the other hand, as previously indicated, the formation times of X^- and 2X are much longer and yield 55 ps and 80 ps, respectively. To provide a consistent interpretation of the observed differences in the formation dynamics, we first note that fast formation of the neutral exciton clearly indicates the rapidity of the interdot transfer. Consequently, much slower formation of the X^- and 2X has to be induced by some additional phenomenon, which takes place during the energy relaxation rather than the transfer itself. This phenomenon is clearly related to the interaction between the electrons, since the complexes exhibiting fast formation dynamics (X and X^+) contain only single electrons, while complexes characterized by slow dynamics (X^- and 2X) accommodate two electrons in the lowest s shell.

The crucial factor in the electron interaction leading to a slowdown of the formation process is the spin, which is

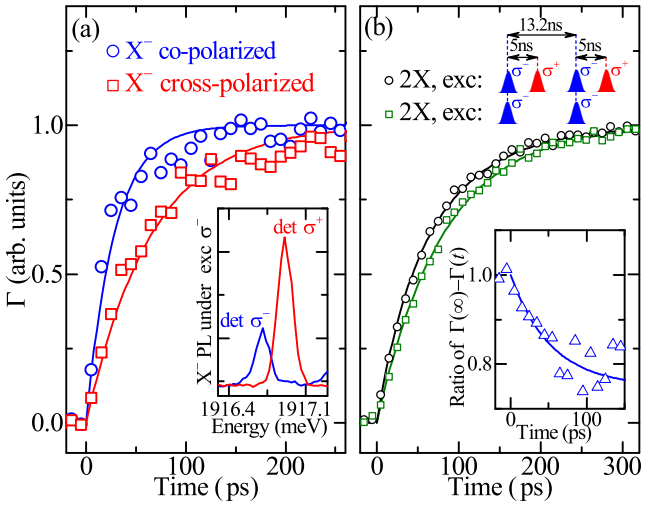

FIG. 4. (Color online) Normalized integrated formation probabilities Γ versus time t after a laser pulse arrival ($B = 1.5$ T). (a) $\Gamma(t)$ for X^- measured under σ^- polarized excitation and detected in two opposite circular polarizations (as indicated). Solid lines represent the fitted curves of the form $\Gamma(t) \propto 1 - \exp(-t/\tau^{\mathrm{exc}})$ with τ^{exc} for co-polarization and cross-polarization of 28 ps and 65 ps, respectively. Inset: the corresponding time-integrated X^- PL spectra. (b) $\Gamma(t)$ for 2X obtained with the use of two excitation protocols (as indicated). Inset: the ratio of $\Gamma(\infty) - \Gamma(t)$ determined under double and single pulse excitation. The solid lines in both plots correspond to the model calculation described in the text.

evidenced by the data displayed in Fig. 4(a). The presented plot shows that X^- formation dynamics is different depending on the polarization of emitted photon and thus on the spin of formed charged exciton. The pronounced difference between the dynamics obtained in co-circular and cross-circular polarization arises due to different spin relaxation paths of the electron pair probed in the two cases. In particular, cross-polarized X^- is formed via simultaneous spin flip of the electron and the hole (i.e., flip flop), which occurs when the electron of the optically injected exciton encounters a resident electron of the same spin orientation. In such a case, the electron-hole flip-flop process constitutes the most efficient spin relaxation path, which leads to negative optical orientation of X^- [see inset to Fig. 4(a)], observed previously in a number of QD systems [27,37–40]. Although the mentioned relaxation of a spin-blockaded electron pair is assisted by a hole, it is still significantly slower than the relaxation of two electrons of antiparallel spins, which gives rise to about two times faster formation dynamics of X^- obtained in the co-polarization.

In general, similar spin-blockade effect could also arise for two holes, as observed, for example, in InGaAs/GaAs QDs [41,42]. However, in our experiment there is no difference between X and X^+ formation dynamics [Fig. 3(b)], which indicates that relaxation of a spin-blockaded pair of holes is a very fast process in the studied CdTe/ZnTe QDs.

In the light of the presented results we expect that slow 2X formation dynamics is caused by the electron spin blockade. However, spin-singlet structure of the 2X ground state implies that regardless of the detected polarization, the 2X PL always reflects the formation dynamics of the same 2X state. Consequently, the spin-related effects in the 2X formation cannot be studied in a similar manner as for the X^-. Instead, we employ two excitation protocols, which differ in the polarization of consecutive pulses. In both cases, the pulse power is set to a value that assures that biexcitons are formed almost exclusively from resident dark excitons. As discussed in Sec. III, we assume that the spin of the electron forming such a dark exciton is preserved during the transfer, and thereby defined by the circular polarization of the corresponding laser pulse. In the first excitation protocol, the QD is simply excited with a train of σ^- polarized pulses separated by 13.2 ns. In such a case, each 2X is formed from two excitons injected by pulses of the same polarization, which entails the same spin orientation of both electrons always leading to the spin-blockade effect. Such a physical picture is modified when using the second excitation protocol, in which the single pulses are replaced with pairs of cross-circularly polarized pulses separated by about 5 ns. Under such excitation, the two excitons from which the 2X is formed may be injected by pulses of different polarizations. This implies that the electron spin blockade will not always occur. This should finally lead to a faster 2X formation dynamics, which is indeed observed experimentally, as presented in Fig. 4(b).

The observed difference between the 2X formation dynamics under two excitation protocols is subtle, however, it is systematically reproducible. Its small amplitude stems from the low pulse power used in our experiment, which corresponds to a negligible probability that two consecutive pulses are absorbed. Consequently, in the second excitation protocol the spin of the electron forming the resident DX can be regarded as random with respect to the spin of the subsequently injected electron. Such an electron pair (prior to its complete relaxation to the s shell) will thus form one out of four possible excited states with equal probabilities: three triplet states (T) or one singlet (S^*). Therefore, only 25% of the 2X formation events under double pulse excitation correspond to fast electron pair spin relaxation from the S^* state. As a result, the actual time-dependent integrated 2X formation probability in such a case reads $\Gamma(t) \propto 1 - \frac{3}{4}\exp(-t/\tau_T) - \frac{1}{4}\exp(-t/\tau_{S^*})$, where τ_T and τ_{S^*} denote the relaxation times of an excited electron pair in triplet and singlet states, respectively. Bearing in mind that under single pulse excitation $\Gamma(t) \propto 1 - \exp(-t/\tau_T)$, the ratio of $\Gamma(\infty) - \Gamma(t)$ determined with the use of two excitation protocols should be given by $\frac{3}{4} + \frac{1}{4}\exp(-t/\tau_{S^*} + t/\tau_T)$. This formula aptly reproduces the actual experimental data presented in the inset to Fig. 4(b). The time constant determined from the fit together with the characteristic 2X formation time obtained under single pulse excitation enable us to independently determine $\tau_{S^*} = 30 \pm 10$ ps and $\tau_T = 80 \pm 10$ ps. The former time is almost equal to the fast co-polarized X^- formation time. On the other hand, τ_T is slightly longer compared to the slow X^- formation time of about 65 ps obtained in the cross-polarization. This is related to the fact that cross-polarized X^- is formed via the relaxation of the spin-blockaded electron pair assisted by a single hole, while the two holes forming the 2X are rapidly accommodated in the lowest s shell (as evidenced by the fast X^+ formation dynamics) and does not interact with the electrons. For this reason, the τ_{S^*} and τ_T determined based on the 2X formation dynamics might be regarded as spin

relaxation times of an isolated electron pair in a CdTe QD. Moreover, a good overall agreement between the model and experiment can be also treated as an *ex post* confirmation of the invoked electron spin conservation during the interdot transfer.

It is noteworthy that the rather long relaxation time of an electron pair in the excited singlet state S^* is actually consistent with the results of the previous PL studies of a doubly negatively charged exciton (X^{2-}) in CdTe/ZnTe QDs [43]. The X^{2-} PL spectrum consists of emission lines originating from the recombination to both singlet and triplet states of an excited electron pair. In each case, the linewidth of the PL lines was found to be below the experimental resolution, providing a lower bound of about 10 ps for both τ_{S^*} and τ_T.

V. CONCLUSIONS

Based on the measurements of X and 2X PL intensity dependence on the excitation power we have directly demonstrated contributions of two mechanisms of the 2X formation: either from an empty dot by capture of two electron-hole pairs within a single excitation pulse or from a resident dark exciton created earlier. The latter 2X formation mechanism was shown to be a dominant one in a wide range of excitation powers in the studied CdTe/ZnTe QDs. This finding provides a natural explanation for subquadratic 2X PL intensity power dependence typically observed in many QD systems [7,11–18]. It is also a general example of the importance of the dark exciton state, which is often neglected [7,28], however should be taken into account in the rate-equation models to correctly describe the QD physics under various excitation regimes, including the CW excitation.

The dark-exciton-related 2X formation mechanism evidenced in our work allows us to create the single 2X with the use of two subsequent laser pulses of various polarizations. By exploiting this possibility, we have studied the impact of a carrier spin-blockade effect on the 2X formation dynamics in the time-resolved experiments. Their results, as well as the measured formation dynamics of other excitonic complexes, revealed that the 2X formation in a CdTe/ZnTe QD is slowed down due to the relatively long relaxation time of a spin-blockaded electron pair, while the spin-blockaded holes were shown to rapidly relax to their ground state within less than 14 ps. Our analysis allowed us to estimate the relaxation times of an excited electron pair in singlet and triplet states to be about 30 ± 10 ps and 80 ± 10 ps, respectively.

ACKNOWLEDGMENTS

This work was supported by the Polish Ministry of Science and Higher Education in years 2012–2016 as research grant "Diamentowy Grant"; by the Polish National Science Centre under decisions DEC-2011/02/A/ST3/00131 and DEC-2012/07/N/ST3/03130; and by the Foundation for Polish Science (FNP) subsidy "Mistrz". Project was carried out with the use of CePT, CeZaMat, and NLTK infrastructures financed by the European Union - the European Regional Development Fund within the Operational Programme "Innovative economy" for 2007–2013.

[1] P. Michler, A. Kiraz, C. Becher, W. V. Schoenfeld, P. M. Petroff, L. Zhang, E. Hu, and A. Imamoglu, A quantum dot single-photon turnstile device, Science **290**, 2282 (2000).

[2] P. Michler, A. Imamoglu, M. D. Mason, P. J. Carson, G. F. Strouse, and S. K. Buratto, Quantum correlation among photons from a single quantum dot at room temperature, Nature (London) **406**, 968 (2000).

[3] C. Santori, M. Pelton, G. Solomon, Y. Dale, and Y. Yamamoto, Triggered single photons from a quantum dot, Phys. Rev. Lett. **86**, 1502 (2001).

[4] D. V. Regelman, U. Mizrahi, D. Gershoni, E. Ehrenfreund, W. V. Schoenfeld, and P. M. Petroff, Semiconductor quantum dot: A quantum light source of multicolor photons with tunable statistics, Phys. Rev. Lett. **87**, 257401 (2001).

[5] E. Moreau, I. Robert, L. Manin, V. Thierry-Mieg, J. M. Gérard, and I. Abram, Quantum cascade of photons in semiconductor quantum dots, Phys. Rev. Lett. **87**, 183601 (2001).

[6] J. Persson, T. Aichele, V. Zwiller, L. Samuelson, and O. Benson, Three-photon cascade from single self-assembled InP quantum dots, Phys. Rev. B **69**, 233314 (2004).

[7] J. Suffczyński, T. Kazimierczuk, M. Goryca, B. Piechal, A. Trajnerowicz, K. Kowalik, P. Kossacki, A. Golnik, K. P. Korona, M. Nawrocki, J. A. Gaj, and G. Karczewski, Excitation mechanisms of individual CdTe/ZnTe quantum dots studied by photon correlation spectroscopy, Phys. Rev. B **74**, 085319 (2006).

[8] M. Bayer, G. Ortner, O. Stern, A. Kuther, A. A. Gorbunov, A. Forchel, P. Hawrylak, S. Fafard, K. Hinzer, T. L. Reinecke, S. N. Walck, J. P. Reithmaier, F. Klopf, and F. Schäfer, Fine structure of neutral and charged excitons in self-assembled In(Ga)As/(Al)GaAs quantum dots, Phys. Rev. B **65**, 195315 (2002).

[9] P. Michler, *Single Semiconductor Quantum Dots* (Springer, Heidelberg, 2009).

[10] M. Grundmann and D. Bimberg, Theory of random population for quantum dots, Phys. Rev. B **55**, 9740 (1997).

[11] M. Benyoucef, S. M. Ulrich, P. Michler, J. Wiersig, F. Jahnke, and A. Forchel, Enhanced correlated photon pair emission from a pillar microcavity, New J. Phys. **6**, 91 (2004).

[12] M. Reischle, G. J. Beirne, R. Roßbach, M. Jetter, and P. Michler, Influence of the dark exciton state on the optical and quantum optical properties of single quantum dots, Phys. Rev. Lett. **101**, 146402 (2008).

[13] G. Sallen, A. Tribu, T. Aichele, R. André, L. Besombes, C. Bougerol, S. Tatarenko, K. Kheng, and J. P. Poizat, Exciton dynamics of a single quantum dot embedded in a nanowire, Phys. Rev. B **80**, 085310 (2009).

[14] M. E. Reimer, M. P. van Kouwen, A. W. Hidma, M. H. M. van Weert, E. P. A. M. Bakkers, L. P. Kouwenhoven, and V. Zwiller, Electric field induced removal of the biexciton binding energy in a single quantum dot, Nano Lett. **11**, 645 (2011).

[15] J. Gomis-Bresco, G. Muñoz-Matutano, J. Martíez-Pastor, B. Alén, L. Seravalli, P. Frigeri, G. Trevisi, and S. Franchi,

Random population model to explain the recombination dynamics in single InAs/GaAs quantum dots under selective optical pumping, New J. Phys. **13**, 023022 (2011).

[16] K. Kukliński, Ł. Kłopotowski, K. Fronc, M. Wiater, P. Wojnar, P. Rutkowski, V. Voliotis, R. Grousson, G. Karczewski, J. Kossut, and T. Wojtowicz, Tuning the inter-shell splitting in self-assembled CdTe quantum dots, Appl. Phys. Lett. **99**, 141906 (2011).

[17] J. Canet-Ferrer, G. Muñoz-Matutano, J. Herranz, D. Rivas, B. Alén, Y. Gonzalez, D. Fuster, L. Gonzalez, and J. Martíez-Pastor, Exciton and multiexciton optical properties of single InAs/GaAs site-controlled quantum dots, Appl. Phys. Lett. **103**, 183112 (2013).

[18] M. Zieliński, K. Gołasa, M. R. Molas, M. Goryca, T. Kazimierczuk, T. Smoleński, A. Golnik, P. Kossacki, A. A. L. Nicolet, M. Potemski, Z. R. Wasilewski, and A. Babiński, Excitonic complexes in natural InAs/GaAs quantum dots, Phys. Rev. B **91**, 085303 (2015).

[19] K. Kowalik, O. Krebs, A. Golnik, J. Suffczyński, P. Wojnar, J. Kossut, J. A. Gaj, and P. Voisin, Manipulating the exciton fine structure of single CdTe/ZnTe quantum dots by an in-plane magnetic field, Phys. Rev. B **75**, 195340 (2007).

[20] M. A. Dupertuis, K. F. Karlsson, D. Y. Oberli, E. Pelucchi, A. Rudra, P. O. Holtz, and E. Kapon, Symmetries and the polarized optical spectra of exciton complexes in quantum dots, Phys. Rev. Lett. **107**, 127403 (2011).

[21] T. Smoleński, T. Kazimierczuk, M. Goryca, T. Jakubczyk, Ł. Kłopotowski, Ł. Cywiński, P. Wojnar, A. Golnik, and P. Kossacki, In-plane radiative recombination channel of a dark exciton in self-assembled quantum dots, Phys. Rev. B **86**, 241305 (2012).

[22] M. Korkusinski and P. Hawrylak, Atomistic theory of emission from dark excitons in self-assembled quantum dots, Phys. Rev. B **87**, 115310 (2013).

[23] I. Schwartz, E. R. Schmidgall, L. Gantz, D. Cogan, E. Bordo, Y. Don, M. Zielinski, and D. Gershoni, Deterministic writing and control of the dark exciton spin using single short optical pulses, Phys. Rev. X **5**, 011009 (2015).

[24] M. Zieliński, Y. Don, and D. Gershoni, Atomistic theory of dark excitons in self-assembled quantum dots of reduced symmetry, Phys. Rev. B **91**, 085403 (2015).

[25] Y. Léger, L. Besombes, L. Maingault, and H. Mariette, Valence-band mixing in neutral, charged, and Mn-doped self-assembled quantum dots, Phys. Rev. B **76**, 045331 (2007).

[26] T. Kazimierczuk, T. Smoleński, M. Goryca, Ł. Kłopotowski, P. Wojnar, K. Fronc, A. Golnik, M. Nawrocki, J. A. Gaj, and P. Kossacki, Magnetophotoluminescence study of intershell exchange interaction in CdTe/ZnTe quantum dots, Phys. Rev. B **84**, 165319 (2011).

[27] T. Kazimierczuk, J. Suffczyński, A. Golnik, J. A. Gaj, P. Kossacki, and P. Wojnar, Optically induced energy and spin transfer in nonresonantly coupled pairs of self-assembled CdTe/ZnTe quantum dots, Phys. Rev. B **79**, 153301 (2009).

[28] T. Kazimierczuk, M. Goryca, M. Koperski, A. Golnik, J. A. Gaj, M. Nawrocki, P. Wojnar, and P. Kossacki, Picosecond charge variation of quantum dots under pulsed excitation, Phys. Rev. B **81**, 155313 (2010).

[29] B. Pietka, J. Suffczyński, M. Goryca, T. Kazimierczuk, A. Golnik, P. Kossacki, A. Wysmolek, J. A. Gaj, R. Stepniewski, and M. Potemski, Photon correlation studies of charge variation in a single GaAlAs quantum dot, Phys. Rev. B **87**, 035310 (2013).

[30] M. Goryca, T. Kazimierczuk, M. Nawrocki, A. Golnik, J. A. Gaj, P. Kossacki, P. Wojnar, and G. Karczewski, Optical manipulation of a single Mn spin in a CdTe-based quantum dot, Phys. Rev. Lett. **103**, 087401 (2009).

[31] M. Koperski, M. Goryca, T. Kazimierczuk, T. Smoleński, A. Golnik, P. Wojnar, and P. Kossacki, Introducing single Mn^{2+} ions into spontaneously coupled quantum dot pairs, Phys. Rev. B **89**, 075311 (2014).

[32] M. Goryca, M. Koperski, P. Wojnar, T. Smoleński, T. Kazimierczuk, A. Golnik, and P. Kossacki, Coherent precession of an individual 5/2 Spin, Phys. Rev. Lett. **113**, 227202 (2014).

[33] O. Labeau, P. Tamarat, and B. Lounis, Temperature dependence of the luminescence lifetime of single CdSe/ZnS quantum dots, Phys. Rev. Lett. **90**, 257404 (2003).

[34] R. Shen, H. Mino, G. Karczewski, T. Wojtowicz, J. Kossut, and S. Takeyama, Biexciton formation induced by bright-dark exciton transitions in a diluted magnetic semiconductor asymmetric quantum well, J. Lumin. **112**, 204 (2005).

[35] S. Bounouar, C. Morchutt, M. Elouneg-Jamroz, L. Besombes, R. André, E. Bellet-Amalric, C. Bougerol, M. Den Hertog, K. Kheng, S. Tatarenko, and J. P. Poizat, Exciton-phonon coupling efficiency in CdSe quantum dots embedded in ZnSe nanowires, Phys. Rev. B **85**, 035428 (2012).

[36] T. Smoleński, T. Kazimierczuk, M. Goryca, P. Kossacki, J. A. Gaj, P. Wojnar, K. Fronc, M. Korkusiński, and P. Hawrylak, Influence of configuration mixing on energies and recombination dynamics of excitonic states in CdTe/ZnTe quantum dots, Acta Phys. Pol. A **119**, 615 (2011).

[37] S. Cortez, O. Krebs, S. Laurent, M. Senes, X. Marie, P. Voisin, R. Ferreira, G. Bastard, J.-M. Gérard, and T. Amand, Optically driven spin memory in *n*-doped InAs-GaAs quantum dots, Phys. Rev. Lett. **89**, 207401 (2002).

[38] S. Laurent, M. Senes, O. Krebs, V. K. Kalevich, B. Urbaszek, X. Marie, T. Amand, and P. Voisin, Negative circular polarization as a general property of *n*-doped self-assembled InAs/GaAs quantum dots under nonresonant optical excitation, Phys. Rev. B **73**, 235302 (2006).

[39] I. A. Akimov, D. H. Feng, and F. Henneberger, Electron spin dynamics in a self-assembled semiconductor quantum dot: The limit of low magnetic fields, Phys. Rev. Lett. **97**, 056602 (2006).

[40] Y. Benny, R. Presman, Y. Kodriano, E. Poem, D. Gershoni, T. A. Truong, and P. M. Petroff, Electron-hole spin flip-flop in semiconductor quantum dots, Phys. Rev. B **89**, 035316 (2014).

[41] E. Poem, Y. Kodriano, C. Tradonsky, B. D. Gerardot, P. M. Petroff, and D. Gershoni, Radiative cascades from charged semiconductor quantum dots, Phys. Rev. B **81**, 085306 (2010).

[42] E. Poem, Y. Kodriano, C. Tradonsky, N. H. Lindner, B. D. Gerardot, P. M. Petroff, and D. Gershoni, Accessing the dark exciton with light, Nature Phys. **6**, 993 (2010).

[43] T. Kazimierczuk, T. Smoleński, J. Kobak, M. Goryca, W. Pacuski, A. Golnik, K. Fronc, Ł. Kłopotowski, P. Wojnar, and P. Kossacki, Optical study of electron-electron exchange interaction in CdTe/ZnTe quantum dots, Phys. Rev. B **87**, 195302 (2013).